sustainability

MDPI

Article

Investigating the Resilience of Fiber-Reinforced Clay Under Freeze–Thaw Cycles

Talal Taleb * and Yesim S. Unsever

Department of Civil Engineering, Bursa Uludağ University, Bursa 16059, Turkey; unsever@uludag.edu.tr
* Correspondence: eng.talaltaleb@hotmail.com

Abstract

In cold-region engineering, freeze–thaw (F–T) cycles act as a critical stressor on soil stability, where the recurring transition between frost heave and thaw settlement can drastically alter geotechnical properties and threaten long-term structural integrity. Yet, while the static characteristics of frozen soils are well documented, the dynamic impact of repetitive thermal cycling on long-term soil behavior remains a significant and relatively underexplored challenge in the field. This study investigates the effectiveness of polypropylene fiber (FPP) as a sustainable and environmentally benign reinforcement for high-plasticity clay. The research examines FPP's influence on stress–axial strain relationships (unconsolidated undrained (UU) compressive strength) and its ability to mitigate frost heave and volumetric changes during F–T cycles. Laboratory-prepared FPP–clay samples were subjected to ten closed-system F–T cycles and tested using a UU triaxial machine. Results showed a 51% decrease in UU strength for unreinforced samples after ten cycles, while samples reinforced with 1% FPP exhibited only an 18.4% reduction. FPP reinforcement reduced frost heave and thaw settlement by 30% and significantly enhanced UU strength, increasing it by 60% before F–T cycles and 167% after exposure. The findings highlight FPP's effectiveness in improving soil strength, minimizing volumetric changes, and mitigating frost-related damage, making it a viable solution for enhancing soil performance in cold regions.

Keywords: UU triaxial strength; fiber-reinforced soil; failure strength; freeze–thaw cycles; secant modulus

1. Introduction

Freeze–thaw cycles significantly affect the engineering properties of clayey soils in cold regions. These cycles can modify the soil's behavior and characteristics. Clayey soils, particularly those rich in minerals like montmorillonite and illite, are highly prone to swelling and shrinkage, which can lead to the development of cracks and compromise the soil's stability and strength. The development and progression of cracks in cover and liner structures can create preferential water flow paths, significantly increasing hydraulic conductivity and ultimately causing the failure of drainage systems in dam constructions. As soil undergoes the freezing process, ice crystals of varying shapes and sizes disperse throughout the soil, contributing to the formation of a range of structures such as ice lenses, segregated ice, and frost heaves, which influence soil stability and engineering properties (Hohmann Porebska [1]). However, when the defrosting phase begins, both the top and bottom parts of the frozen layer thaw out. This results in significant alterations in how soil behaves.

Check for updates

Academic Editor: Castorina Silva Vieira

Received: 22 February 2026
Revised: 21 March 2026
Accepted: 24 March 2026
Published: 26 March 2026

Copyright: © 2026 by the authors. Licensee MDPI, Basel, Switzerland. This article is an open access article distributed under the terms and conditions of the Creative Commons Attribution (CC BY) license.

As expansive soils are commonly employed in the liners and slurry wall construction for waste containment, freezing–thawing cracking can have a large impact on these structures and their functionality (Miller et al. [2]). In other words, the existence of fissures or cracks suggests that groundwater recharge may outpace the drawdown of exposed terrain, potentially resulting in slope instability and reduced bearing capacity of foundations (Baker [3]; Silvestri et al. [4]). Therefore, proposing a suitable technical solution for resisting environmental changes is always mandatory, specifically in frozen regions, where the stability and durability of the technical solution provided for soil subjected to cyclical freezing and thawing conditions come as a priority (Ghazavi and Roustaei [5]; Roustaei et al. [6]).

Numerous studies have focused on enhancing traditional treatment approaches by suggesting novel additives, materials and methods to solidify clayey soils and reduce the negative impacts linked with them. Each of these approaches may encounter challenging circumstances that hinder their sustainability and ability to withstand environmental impacts, as well as prove costly due to the use of expensive materials. Consequently, ongoing research focuses on exploring alternative methods that enhance mechanical properties, minimize volume fluctuations, and improve other engineering characteristics of clayey soils by incorporating various additives or reinforcing materials (Akbulut et al. [7]; Raddi M. AlZubaidi et al. [8]; Ahmed M. Al-Mahbashi et al. [9]; Abdullah A. Sharo et al. [10]; Mohammed A. M. Al-Bared et al. [11]; Farghaly A. et al. [12]). However, the majority of these approaches do not handle clayey soil behavior under frost heaving and cyclic freezing–thawing. Thus, new methods and materials are still required to be presented to reduce volumetric strain-related clayey soil movements and resist the added stress imposed on by seasonal temperature variations, particularly freeze–thaw (F–T) cycles. Also, the new stabilizing materials' cost should addressed in the overall evaluations of new treatment methods or proposals.

Recently, fiber-based materials have been introduced as soil stabilizers to enhance the strength of problematic soils. Many investigations have been conducted on fiber–soil mixtures (Akbulut et al. [7]; Kumar et al. [13]; Sivakumar Babu et al. [14]; Viswanadham et al. [15]). The findings of prior studies suggest a correlation between the fiber content and the strength or mechanical characteristics of fiber–soil mixtures. According to the findings of Tang et al. [16], the tensile strength demonstrated an upward trend as the amount of fiber inclusions increased. Taleb and Unsever [17,18] revealed that the inclusion of fibers resulted in an enhancement of unconfined compressive strength, while simultaneously reducing the swell pressure and volumetric changes caused by the desiccation process. On the other hand, limited research has been conducted regarding soil additives and their combinations to assess their impact on freeze–thaw resistance, as well as their dynamic and static behavior. However, soil strength change investigations due to intense climatic variations are essential, especially for earthworks purposes. Results of previous studies showed that clayey soils were more affected by freeze–thaw cycles than granular soils (Aldaood et al. [19]; Ling et al. [20]). Thus, in cold regions, changes in soil strength characteristics should be considered in the design, construction, and service-life stages. Boz and Sezer [21] as well as Ding et al. [22] observed in their respective studies that various soils experience a substantial decrease in their physical properties and strength parameters when exposed to (F–T) cycles. Zhang et al. [23,24] determined that destruction in pavement structures can be observed due to the frost heave caused by temperature changing. Therefore, various types of additives (physical and chemical additives) should be employed to confront these destructive impacts. Synthetic and natural fibers are the most customarily used additives to enhance the mechanical behavior (Hejazi et al. [25]). The impact of the geogrid-reinforcing technique on silty clay soils undergoing (F–T) cycles,

along with its effects on thaw-settlement and frost-heave deformities, was examined by Zhao et al. [26]. Several other studies have concentrated on investigating the impacts of freeze–thaw (F–T) cycles on soils that have been stabilized using polymeric fluids (Soltani-Jigheh and Azarnia [27]; Krainiukov et al. [28]), chemicals (Eskisar et al. [29]), physical additives (Zaimoglu [30]; Ghazavi and Roustaie [31]; Orakoglu and Liu [32]; Kravchenko et al. [33]), nano-materials (Yarbasi et al. [34]; Kalkan [35]; Ahmadi et al. [36]), and combinations of additive materials, both physical and chemical in nature (Jafari and Esna-ashari [37]; Ding et al. [22]; Gao et al. [38]). Evidently, the adverse consequences resulting from (F–T) cycles of the mentioned materials were mitigated.

Nevertheless, it is crucial to recognize the significant environmental impact of using chemical additives for soil stabilization, as this process often leads to the release of large amounts of greenhouse gases into the atmosphere during a pronounced alkalization stage (as observed in the case of lime treatment); consequently, such outcomes can result in substantial societal expenses and pose a potential risk to the biota and plant life (Rogers et al. [39]). Similarly, the production stage of fly ash and cement emits significant quantities of CO2, hindering plant growth and causing environmental pollution (Caravaca et al. [40]; El-Attar et al. [41]). Hence, prioritizing the utilization of environmentally friendly and sustainable alternatives is crucial to bolster mechanical resilience and withstand the added strain caused by freeze–thaw cycles or temperature differentials. Although previous studies have explored various methods of soil stabilization, limited research has specifically focused on the use of polypropylene fibers in clayey soils subjected to freeze–thaw (F–T) cycles. In particular, studies focusing on high-plasticity clay and simultaneously evaluating both mechanical behavior and volumetric response under repeated freeze–thaw cycles remain limited. In a broader material context, similar reinforcement mechanisms have been extensively investigated in high-performance composites, where the integration of nano-additives and fibers has been shown to mitigate damage under freeze–thaw and salt erosion conditions by densifying the internal structure, while the overall toughness is largely governed by the quality of the fiber–matrix interface bonding (Zhaoxia Hu. et al. [42]; Zhijie Liu et al. [43]). However, these findings are primarily derived from concrete-based materials, and comparable investigations in fiber-reinforced soils remain limited. Thus, they provide indicative insight into general fiber-reinforcement behavior rather than direct evidence for soil systems. Drawing from these principles, this study focuses on assessing the effectiveness of polypropylene fibers in enhancing the mechanical and volumetric performance of high-plasticity clayey soils subjected to repeated freeze–thaw cycles.

The novelty of this study lies in its exploration of polypropylene fibers as a cost-effective and environmentally friendly solution to enhance the strength and durability of clayey soils under repeated (F–T) cycles. The study evaluates the viability of polypropylene fibers to enhance mechanical performance (UU triaxial strength, secant modulus) and volumetric behavior (frost heave and thaw settlement), addressing a gap in previous research. It further investigates the influence of fiber inclusion to determine the optimal dosage for maximum enhancement, highlighting the durability and effectiveness of fiber reinforcement under repeated F–T cycles. Ultimately, this study holds significant importance as it contributes to advancing sustainable soil stabilization practices, offering insights into the effectiveness of polypropylene fiber in strengthening clayey soils against freeze–thaw-induced stresses. By filling this research gap, the study provides valuable data that could guide the adoption of polypropylene fibers in real-world applications, paving the way for more resilient and eco-conscious infrastructure development. By elucidating the mechanics and durability of fiber-reinforced soil, this research could inform future endeavors in infrastructure development and environmental conservation, fostering resilient and eco-conscious engineering solutions.

2. Materials and Methods

2.1. Polypropylene Fiber

Polypropylene fiber (FPP) is a flexible thermoplastic material that undergoes a controlled polymerization process to produce different commercial forms under specific heat and pressure conditions. FPP is present in two distinct forms: "isotactic," denoting the crystallizable form (utilized in this study), and "atactic," representing the non-crystallizable form (Brown et al. [44]). Table 1 presents the key properties of the FPP used, as stated on the manufacturer's provided identification card. Figure 1 shows the material utilized.



Figure 1. Used polypropylene fiber.

Table 1. Used polypropylene fiber (FPP)'s properties.

Fiber's Properties	Values
Type	Single fiber
Unit weight	0.91 g/cm^3
Diameter on average	0.034 mm
Length on average	12 mm
Tensile strength at break point	350 MPa
Unit weight	0.91 g/cm^3

Polypropylene is among the most recyclable thermoplastics, capable of being re-melted and repurposed for various applications, including fiber production. The recycling process is highly energy-efficient, consuming significantly less energy than manufacturing new FPP from raw materials, which contributes to a reduced carbon footprint. For instance, producing one ton of recycled FPP prevents approximately one ton of CO_2 emissions compared to the production of virgin FPP, thereby significantly mitigating the environmental impact. Moreover, recycled polypropylene fibers retain mechanical properties comparable to their virgin counterparts, making them suitable for construction and industrial applications, such as concrete reinforcement and geotextiles, where they meet technical performance standards. In addition, recycled polypropylene fibers (FPPs) offer a sustainable alternative to conventional additives such as cement or lime, consuming approximately 70% less energy than virgin polymers and significantly reducing greenhouse gas emissions. Using recycled fibers diverts plastic from landfills and replaces carbon-intensive cement, which accounts for nearly 8% of global CO_2 emissions, thereby supporting circular economy goals. Quantitatively, substituting a typical 10% cement treatment with just 0.5% recycled fiber reinforcement can lower the total CO_2 emissions associated with subgrade improvements by over 90–95% (Rogers et al. [39]). While potential trade-offs, including microplastic concerns and long-term durability, require further investigation, these benefits reduce emissions, minimize plastic waste, and promote a circular economy, underscoring the environmental advantages of incorporating recycled fibers into geotechnical applications (Franklin Associates [45]).

The primary benefits of this fiber lie in its widespread industrial application due to its cost-effectiveness compared to other conventional additives, as well as its inert nature, which prevents absorption or interaction with soil moisture. As reported by Hejazi et al. [25], fiber–soil mixtures offer significant advantages, including availability, economic benefits, and suitability for implementation in any weather conditions. However, achieving uniformity in fiber distribution under field conditions poses significant challenges compared to controlled laboratory mixing, as highlighted by various researchers. Factors such as variability in soil properties and the complexities of large-scale implementation, such as uneven fiber dispersion during road construction or slope stabilization projects, can hinder consistent integration. For instance, field applications often face challenges like ensuring uniform fiber distribution in expansive clay soils used for embankments or addressing compaction variability in landfill covers. However, advanced mixing techniques, such as helical or oscillatory methods suggested by Hejazi et al. [25], offer promising solutions to these issues. Addressing these challenges requires collaborative efforts among engineers, material scientists, and industry professionals to develop practical, cost-effective, and sustainable methods for large-scale fiber integration. Additionally, investing in research and development to optimize processes and tackle logistical hurdles will be pivotal in promoting the widespread adoption of fiber-reinforced soil technologies.

2.2. Clayey Soil Identification

The soil under investigation was obtained from an ongoing project in Gaziantep, Turkey, demonstrating a relatively uniform composition. Before initiating the planned testing program, a series of preliminary experiments were conducted to determine the soil's overall properties. These experiments comprised specific gravity tests, gradation analyses, Atterberg limit tests, and hydrometer analyses. Table 2 summarizes the preliminary test findings.

Table 2. Studied soil characteristics.

Soil Properties	Values
Specific gravity	2.70
Liquid limit (LL)	57%
Plastic limit (PL)	22.67%
Plasticity index (PI)	34.33%
Unified Soil Classification System (USCS)	CH
Optimum moisture content (OMC)	22.5%
Maximum dry density (MDD)	1.57 g/cm^3
Sand (4.75–0.075 mm)	24%
Silt (0.075–0.002 mm)	39%
Clay < 2 μm	35%
Shrinkage limit	12.3%
Maximum swelling strain	16%

3. Laboratory Test Investigations

An experimental program was conducted in the laboratory to assess the potential and effectiveness of FPP in enhancing the characteristics of mechanical strength and durability of clayey soil (CH classification). In order to analyze the strength characteristics, a series of conventional (UU) triaxial tests were performed on fiber-reinforced samples containing three varying fiber inclusion (i.e., by dry weight of the soil, proportions of 0.5%, 1%, and 1.5% were utilized). The stress–strain relationships of the clayey soil were analyzed and compared with unstabilized samples to determine the optimal fiber content that achieves the most significant enhancement rate. For durability assessment, standard UU tests were

performed on fiber-reinforced samples exposed to up to 10 closed-system (F–T) cycles, and the resulting changes in UU strength were compared with those of unreinforced samples. Furthermore, as indicators of durability performance, the changes in volume and the strength reduction due to (F–T) cycles were also computed.

3.1. Sample Preparation

The samples were divided into four groups based on the respective amounts of fiber content (0%, 0.5%, 1%, 1.5%) considered in this study. The maximum fiber content of 1.5% was chosen to ensure soil workability and facilitate the easy formation of samples during testing. Additionally, this limit helps prevent diminishing returns or reduced performance, which can occur with excessive fiber addition due to clustering or decreased cohesion among soil particles. Soil without any treatment was used to form cylindrical specimens sized 80 mm in height and 38 mm in diameter. The samples were compacted using the soil's determined optimum moisture content (OMC) and maximum dry density (MDD) values (i.e., the dry density of the sample corresponds to 1.57 g/cm^3 with a water content of 22.5% for all cases) to facilitate a direct comparison between reinforced and unreinforced samples. This methodology is supported by previous studies (Akbulut et al. [7]; Kumar et al. [13]; Taleb and Unsever [46]) that demonstrated that fiber percentages do not significantly alter the compaction behavior of cohesive materials. Adopting these consistent preparation benchmarks ensures that the observed mechanical enhancements result from fiber–soil interaction rather than variations in the initial compaction state. Specimen tolerances were maintained within $\pm$0.02 g/cm^3 for dry density and $\pm$0.2% for initial moisture content. To achieve the desired MDD, the specimen mold was gradually filled using a step-by-step method that involved layered pouring and static compaction. The mold was filled to a height of 100 mm and a diameter of 38 mm before applying static compaction to ensure uniform density.

The process of mixing fibers with soil, conducted until no visible fiber clusters or agglomerations remained, involved two main steps. Initially, fibers at the designated proportions were manually mixed into the soil together with about 10% water by dry soil weight (about half of the OMC value) to ensure even distribution and prevent clumping. Second, the remaining water needed to reach the OMC was added to the initial fiber–soil mixture to achieve the target moisture content. Subsequently, the mixtures were covered with polyethylene bags and sealed for 72 h to maintain consistent moisture content. Before forming the specimens through compaction in steel molds, the moisture content was checked to ensure it met the desired level. Following completion of the static compaction process, all samples were prepared and made ready for conducting the UU triaxial tests.

3.2. Conventional Undrained Unconsolidated (UU) Triaxial Tests

Unconsolidated specimens underwent standard UU triaxial tests utilizing a strain control device in accordance with ASTM D2850 [47]. The unconsolidated undrained (UU) triaxial test was chosen because it effectively represents short-term loading conditions with restricted drainage, mirroring field situations such as highway embankments, bridge abutments, and subgrade soils in cold regions. The limited drainage condition also simulates rapid loading or seasonal freeze–thaw cycles, enabling an accurate evaluation of both strength and deformation behavior of fiber-reinforced clay under realistic stress conditions. For each of the four specimens (0%, 0.5%, 1%, 1.5%), the specimens were tested at 0.8 mm/min of strain rate with a displacement resolution of 0.01 mm and at a specific confining pressure of 200 kPa with a load cell resolution of 1.0 N. The adopted rate corresponds to 1% axial strain per minute based on the specimen height, ensuring negligible moisture migration and preserving undrained conditions throughout the test ASTM

D2850 [47]. A single confining pressure of 200 kPa was chosen as it represents the vertical effective stress at depths of approximately 10–12 m, typical of highway embankments, bridge abutments, and medium-sized foundations, and provides a relevant stress level for subgrade and pavement support in cold regions. This intermediate pressure is also ideal for evaluating freeze–thaw (F–T) effects, as ice lens formation and volumetric changes are more pronounced, whereas very low or high stresses can mask structural responses. Using a consistent 200 kPa enables clear comparison across fiber contents and F–T cycles. Additionally, previous researchers (Shukla [48]; Behzad Isazadeh-Khiav et al. [49]) observed comparable strength behavior between stabilized and unstabilized soils across different confining pressure levels (the resemblance of the stress–strain response under varying confining pressures). Thus, UU triaxial tests were carried out on all samples, with each test performed in triplicate to ensure accuracy and repeatability. The results presented represent the average of the three replicates. It is worth mentioning that the consistent stress–strain responses observed, with minimal variability among replicates, further confirm the uniform distribution of fibers within the samples. Figure 2 illustrates the stress–strain responses of both unreinforced and fiber-reinforced specimens subjected to 200 kPa of confining pressure before the freeze–thaw (F–T) cycles. It is important to note that the maximum strain values vary between cases because the termination condition of the UU test is reached when the specimen shows significant deformation or failure, typically characterized by the attainment of peak shear stress. Peak strength was defined as the maximum deviatoric stress for specimens exhibiting strain-softening behavior. For samples showing strain hardening without a distinct peak, the compressive strength was taken as the deviatoric stress at 15% axial strain, in accordance with ASTM D2850 [47]. Therefore, peak strength was recorded at the maximum deviatoric stress, regardless of the strain at which it occurred for comparison purposes. Meanwhile, to ensure a consistent comparison of deformation resistance (stiffness) across all test groups, the secant modulus was computed at a fixed reference strain of 1%. This dual approach allows for the evaluation of ultimate failure capacity while maintaining a uniform baseline for stiffness indexing. Thus, raw data trends were analyzed by plotting the complete stress–strain curves for all cases—0, 0.5%, 1%, and 1.5%—and all F–T cycles. This provides a transparent visual of stiffness degradation and plastic strain accumulation, with data points recorded at 0.25% strain intervals to ensure high-resolution monitoring across all experimental groups.

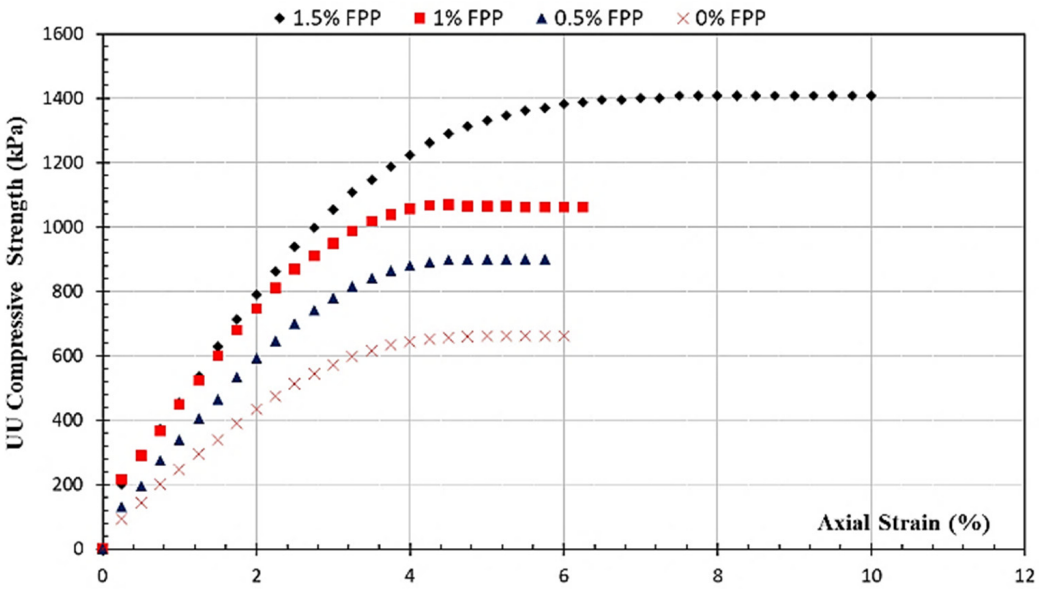


Figure 2. Stress–strain relations under 200 kPa confining pressure before (F–T) cycles.

Furthermore, it was observed during the testing phase that reinforced samples required more time to reach failure compared to unreinforced specimens, with the duration increasing proportionally to the fiber content. Thus, the failure patterns of tested samples with a fiber content of 0%, 0.5%, 1%, and 1.5% are shown in Figure 3. The failure pattern for unreinforced specimens results from linear fracture surfaces distributed over the height of the specimens. Conversely, the fiber-reinforced specimens experienced a gradual extrusion at the middle and bottom sections, leading to a plastic failure characterized by a drum-shaped deformation (confirmed by measuring the diameter at various heights).



Figure 3. Failure patterns with fiber inclusion (from left to right, 0% to 1.5%).

3.3. Conventional Undrained Unconsolidated Triaxial Tests for Specimens Subjected to Freeze–Thaw (F–T) Cycles

The same sampling procedure mentioned earlier was employed, and the prepared specimens were exposed to specific rounds of (F–T) cycles, ranging from 0 to 10, before undergoing UU triaxial testing. The choice of 10 freeze–thaw cycles was based on evidence that the most pronounced changes in soil strength occur early in the freeze–thaw process, with further alterations in cohesion and friction angle tapering off by approximately the tenth cycle (Hong. Y. et al. [50]; M. G. Rosa et al. [51]). This makes 10 cycles a suitable range for capturing the primary degradation behavior. For studies aimed at long-term performance or involving chemical stabilizers, extending beyond 15 cycles has been suggested in the literature (AlFukaha et al. [52]).

For 12 h, the specimens were kept in a temperature-controlled chamber maintained at a constant temperature of −20 °C, followed by approximately 20 °C for the next 12 h to facilitate the thawing period (Figure 4a). This entire 24 h period constituted one cycle. Subsequently, experiments were carried out at room temperature, approximately 20 °C. Following the completion of the (F–T) cycles, variations in physical characteristics and the strength behavior under UU conditions were examined and calculated for both unreinforced and fiber-reinforced soils. Throughout the (F–T) cycle application, the heights and diameters of the samples were measured multiple times. The heights were measured from the bottom surface to the top surface, while the diameters were taken at the midpoint of the height for all measurements. This ensures uniformity and accuracy in measuring the dimensions. Table 3 provides the physical characteristics (height and diameter) of the examined samples following exposure to (F–T) cycles and prior to UU triaxial strength tests. Figure 5 depicts the stress–strain behavior of both fiber-reinforced and unreinforced samples under a confining pressure of 200 kPa following 0, 3, 6, and 10 (F–T) cycles, respectively.



(**a**)



(**b**)



(**c**)

Figure 4. Preparation and testing setup for triaxial experiments: (**a**) Triaxial machine used for testing, (**b**) Soil specimens after testing, and (**c**) Freeze–thaw cabinet employed for sample conditioning.

Table 3. Changes in physical properties after (F–T) cycles and before UU triaxial testing.

Number of (F–T)	Fiber Content (% FPP)	Sample's Height (mm) (h, mm)	Sample's Diameter (D, mm)
0	0%	80	38
	0.5%	80	38
	1%	80	38
	1.5%	80	38

Table 3. *Cont.*

Number of (F–T)	Fiber Content (% FPP)	Sample's Height (mm) (h, mm)	Sample's Diameter (D, mm)
3	0%	84.3	38
	0.5%	84.1	38
	1%	83.7	38
	1.5%	83.6	38
6	0%	85	38.3
	0.5%	84.8	38.2
	1%	84	38.3
	1.5%	84.5	38.3
10	0%	85.3	38.3
	0.5%	84.9	38.3
	1%	84.5	38.3
	1.5%	85	38.3

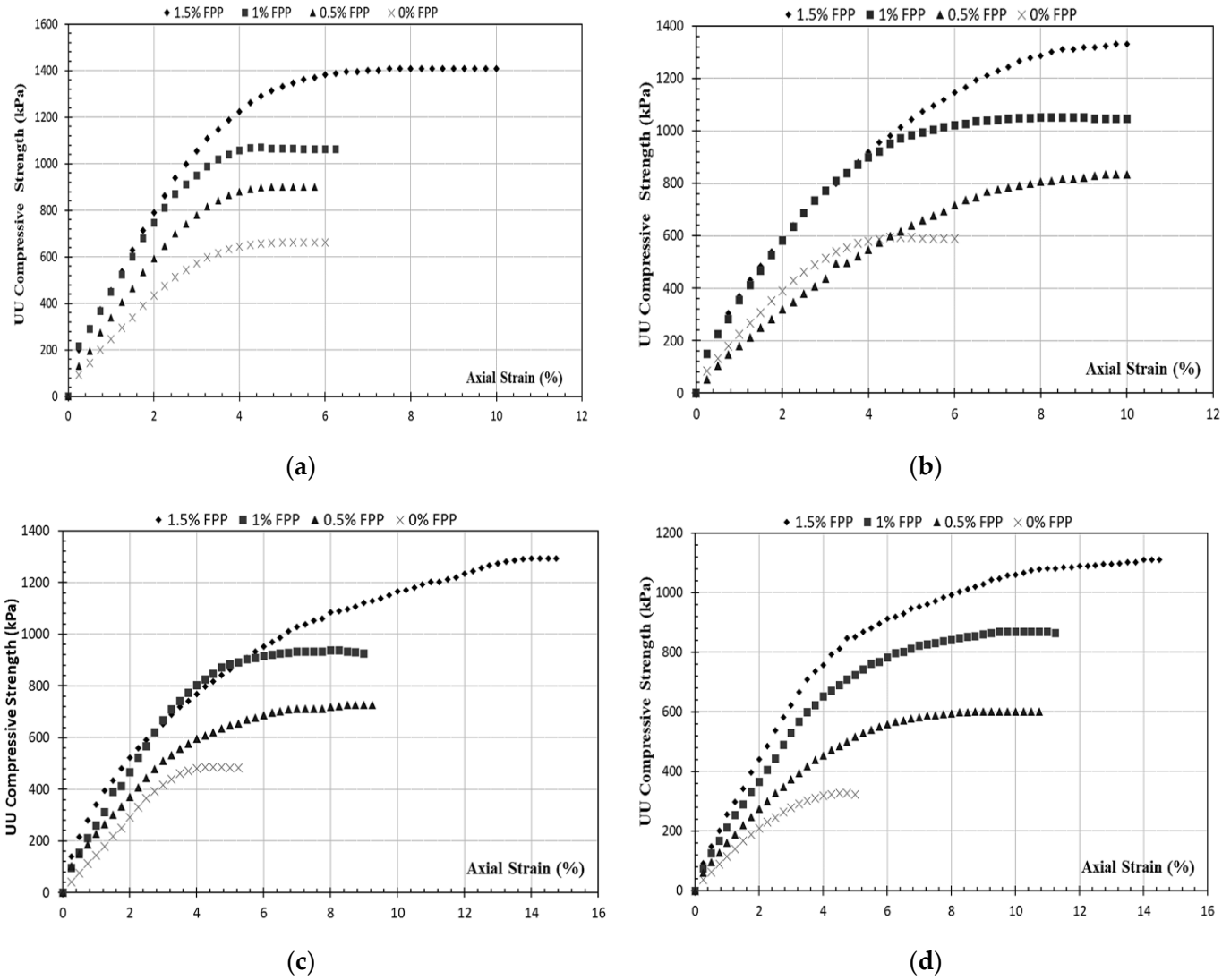
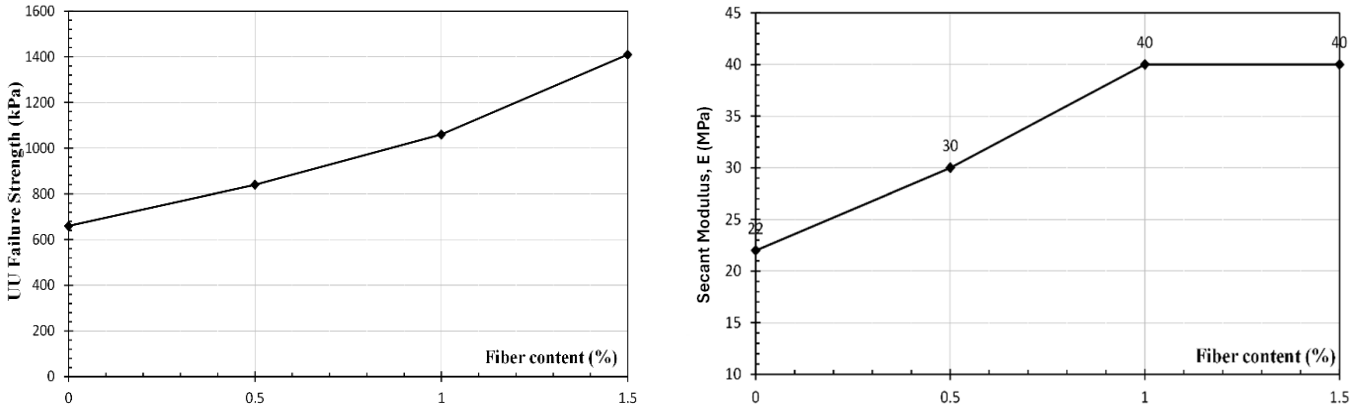


Figure 5. Stress–strain relationships of soil specimens with and without fiber reinforcement (FPP) under different freeze–thaw (F–T) cycles: (**a**) 0 cycles, (**b**) 3 cycles, (**c**) 6 cycles, and (**d**) 10 cycles.

4. Results and Discussions

4.1. Evaluation of Fiber Effect on UU Triaxial Strength Properties (UU Strength and Secant Modulus)

Referring to Figure 2, and by representing the failure strength values for all cases as shown in Figure 6a, a clear steady rise is observed in the UU strength as the fiber inclusion increases. Notably, the strength increased by 35%, 60%, and 112% when incorporating 0.5%, 1%, and 1.5% of fiber, respectively. This can be ascribed to the beneficial fibrous impact, which plays a crucial role in fostering extra interparticle bonds within the soil. It should be noted that microstructural analyses were not performed in this study, so the fiber–soil interaction mechanisms are inferred from macroscopic test results and relative behavior rather than visual observations.



(**a**) (**b**)

Figure 6. UU compressive strength and secant modulus of soil specimens in relation to fiber content: (**a**) UU compressive strength versus fiber content and (**b**) Secant modulus corresponding to fiber content.

To determine the secant modulus, which serves as a key parameter for characterizing deformation resistance and providing an equivalent stiffness index under loading conditions typical of pavement subgrades, the stiffness was evaluated from monotonic UU tests. In this study, the secant modulus was adopted as a proxy for resilient behavior to describe the soil's elasto-plastic response under F–T conditions. It is calculated as the ratio of deviatoric stress to the corresponding axial strain at a fixed strain level of 1%, as expressed by the following equation:

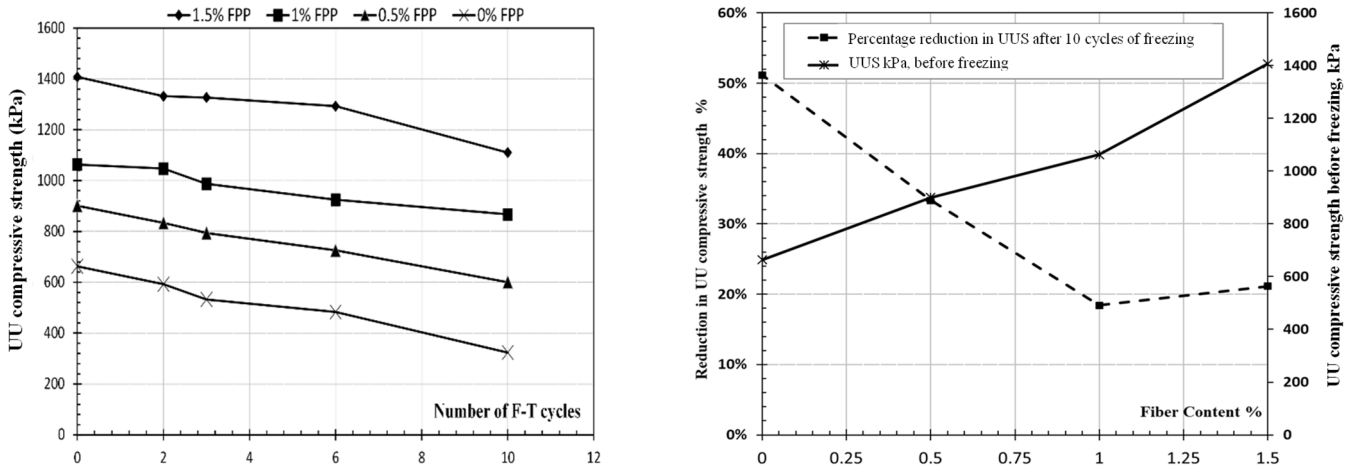
$$E = {}^{\Delta\sigma}/_{\Delta\varepsilon} = \frac{\sigma_{1\%} - \sigma_0}{\varepsilon_{1\%} - \varepsilon_0} \quad (1)$$

where $\Delta\sigma$ represents the increase in deviatoric stress; $\Delta\varepsilon$ represents the increase in deviatoric strain; $\sigma_{1\%}$ is the deviatoric stress associated with the axial strain of 1.0% ($\varepsilon_{1\%}$); and σ_0 and ε_0 are the initial stress and strain respectively (Wang et al. [53]). By representing the E calculations in Figure 6b, it can be observed that E increases with higher fiber content, reaching a maximum value of 40 MPa at 1% and 1.5% fiber inclusion.

4.2. Evaluation the Effect of (F–T) Cycles on UU Triaxial Strength Properties (UU Compressive Strength and Secant Modulus)

Referring to Figure 2, and by representing the failure strength for all cases following 0, 3, 6, and ten (F–T) cycles as illustrated in Figure 7a, it is evident that the strength behavior for all reinforced and unreinforced samples is the same, where for each successive (F–T) cycle, there is a gradual decline in strength; in particular, the unreinforced sample experienced

a reduction in UU strength of up to 51% after undergoing 10 cycles of (F–T). In comparison, the decreasing trend was approximately 33% for the soil reinforced with 0.5% PP fibers, 18.4% for 1% PP fiber reinforcement, and 21.1% for 1.5% PP fiber reinforcement. This behavior can be attributed to the formation of ice during freezing, where soil pore water solidifies and generates forces that disperse soil particles, raising pore water pressure. Throughout this distinctive phase, the presence of ice generates a force that leads to the dispersion of soil particles, resulting in an elevation of pore water pressure. Conversely, throughout the process of thawing, the excessive pore water pressure is unable to revert back to its initial state. Consequently, repeated F–T cycles tend to decrease soil strength (Ghazavi and Roustaie [5]; Wang et al. [53]; Andersland and Ladanyi [54]). This reduction in strength is mainly associated with microstructural changes induced by repeated freeze–thaw (F–T) cycles, including particle rearrangement, aggregation of fine particles, and the formation of microcracks within the soil matrix. These processes progressively loosen the soil fabric and increase porosity, thereby reducing the packing fraction and the interparticle contact area responsible for effective stress transfer. The resulting structural degradation weakens the soil skeleton, explaining the observed decline in undrained strength with increasing F–T cycles in the UU tests. Moreover, repeated F–T cycles promote the formation of larger clay aggregates, which effectively modify particle shape and interparticle interlocking within the soil matrix. These structural changes are consistent with findings in granular material studies, where particle geometry and arrangement strongly influence creep behavior and fluidity (Tong et al. [55] and Zhao et al. [56]). In particular, the altered particle shapes and interlocking patterns govern the evolution of soil stiffness and the accumulation of long-term deformation. Additionally, the reorganization of these aggregates affects the packing density, changing how closely particles are compressed together. Therefore, these changes contribute to the gradual reduction in soil strength and stiffness under repeated environmental loading.



(**a**) (**b**)

Figure 7. UU compressive strength values with varying fiber content (FPP): (**a**) UU compressive strength under different freeze–thaw (F–T) cycles and (**b**) Reduction in UU strength as a function of fiber content.

Consequently, fiber-reinforced samples exhibit a comparatively smaller reduction in strength, as fibers create bridging effects between soil particles and help maintain a more stable internal contact network. This behavior can be attributed to the role of randomly distributed fibers acting as reinforcing elements within the soil matrix, which restrain deformation, delay crack propagation, and enhance resistance to freeze–thaw damage by

maintaining particle connectivity and redistributing stresses within the soil structure. Although numerous studies provide ample evidence, a direct correlation between the number of (F–T) cycles and strength reduction is observed for both fiber-reinforced and unreinforced soils. The highest strength loss was 51% in unreinforced samples, compared to 18.4% with 1% FPP and 21% with 1.5% FPP, indicating that fiber reinforcement reduced frost heave effects by approximately 30%. Thus, a 1% fiber content can be considered optimal for frost heave resistance. However, fiber contents above 1% (i.e., 1.5%) still improve strength but show a diminishing return relative to the incremental material added, indicating a practical threshold beyond which additional fiber does not substantially enhance performance (see Figure 7b). At this optimal level, fibers provide adequate tensile strength and create a matrix that enhances the soil's structural integrity without significantly reducing cohesion. They bridge soil particles, reducing voids and distributing stress evenly, which prevents localized failure during freeze–thaw cycles. Maintaining 1% fiber content inhibits water migration to freezing fronts, minimizing ice lens formation. Additionally, at this percentage, fibers synergistically interact with soil particles to promote interlocking, enhancing stability and resistance to frost heave. Figure 7b presents a compelling observation, showcasing that increasing fiber content significantly mitigates strength loss during F–T cycles.

For assessing the impact of (F–T) cycles on the secant modulus (E), which was calculated for both fiber-stabilized and unstabilized samples that were subjected to a maximum of 10 closed-system (F–T) cycles. Figure 8 illustrates the reduction in secant modulus as the number of (F–T) cycles increases. This reduction is consistent with the previously discussed microstructural degradation caused by repeated freezing and thawing, including increased porosity and weakened interparticle contacts. However, the reinforced samples exhibited smaller reductions in secant modulus, with higher fiber contents corresponding to improved stiffness retention due to the bridging effect of fibers and their ability to maintain a more stable particle network within the soil matrix.

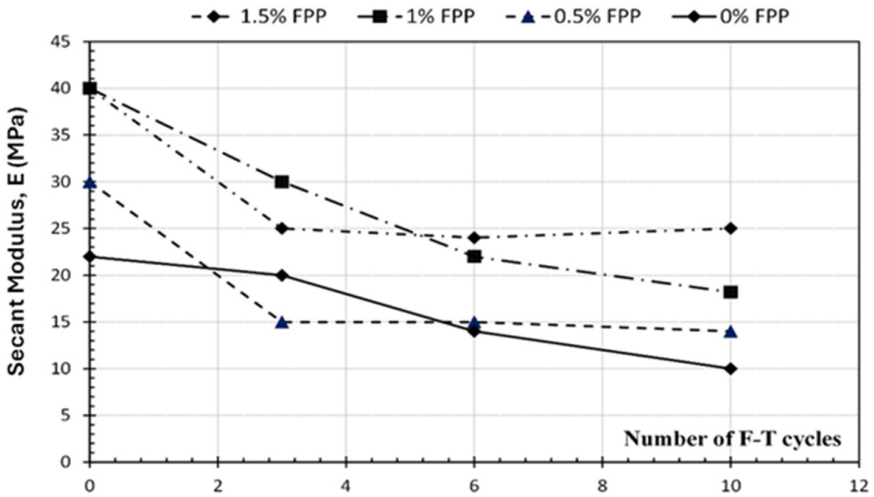


Figure 8. Secant modulus values of soil specimens with varying fiber content (FPP) under different freeze–thaw (F–T) cycles.

4.3. Evaluate the Impact of (F–T) Cycles on Physical Properties (Unit Weight Change Resistance)

Referring to Table 3, it is evident that sample dimensions (i.e., volume) increase progressively with the number of (F–T) cycles for both reinforced and unreinforced cases. Nonetheless, the reinforced samples showed much less volumetric change than the unreinforced ones. This can be explained by the fibers forming bonding forces (coupling forces) that tie soil particles together, minimizing volumetric changes in the reinforced samples. Thus, the variation in specimen height during F–T cycles can be described as

follows: during the thawing stage, ice crystals formed in the freezing stage melt, and the water produced moves downward due to gravity, causing the sample's height to increase (Ghazavi and Roustaie [5]; Wang et al. [53]; Andersland and Ladanyi [54]).

As shown in Figure 9, the alteration in sample height impacts the unit weight (weight per unit volume). Consequently, the unit weight decreases despite the inclusion of FPP. However, the fibers effectively resist greater changes in unit weight compared to the unreinforced samples. Following the ten (F–T) cycles, the unreinforced sample experiences a unit weight reduction approximately 0.9% higher than that of the FPP-reinforced samples. These findings closely align with the results reported by Wang et al. [53].

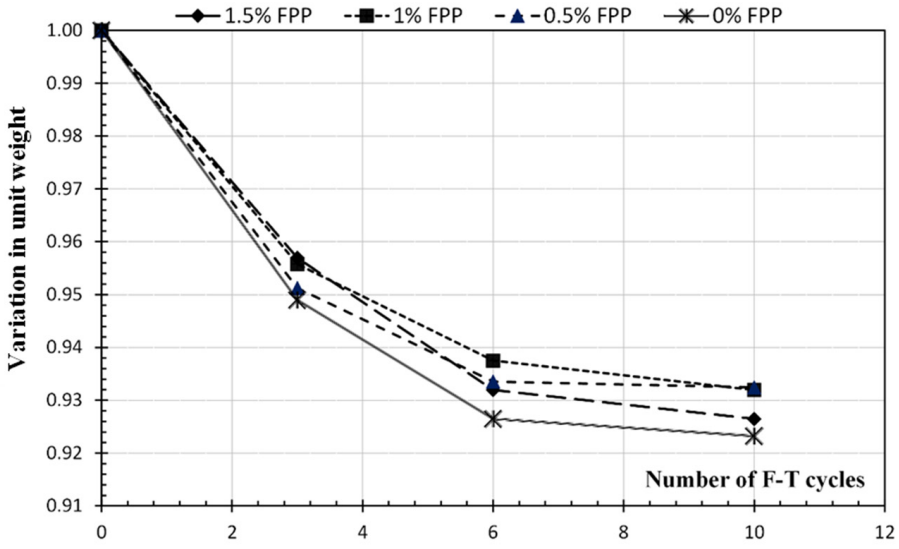


Figure 9. Variation in unit weight of soil specimens with fiber content (FPP) under different freeze–thaw (F–T) cycles.

5. Conclusions

This study demonstrates the positive impact of adding polypropylene fiber (FPP) to high-plasticity clayey soil, significantly enhancing the unconsolidated undrained (UU) triaxial strength properties. The results indicate a substantial increase in strength, with a 112% improvement observed at 1.5% fiber inclusion under a confining pressure of 200 kPa. Additionally, the secant modulus increased by approximately 80% at this reinforcement level. These findings are consistent other studies (Taleb and Unsever [17]; Wei et al. [57]) reporting similar improvements in shear strength and deformation characteristics with fiber reinforcement in clayey soils. Moreover, research by Consoli et al. [58] supports the correlation between fiber inclusion and increased secant modulus, confirming that fiber-reinforced soils exhibit improved mechanical properties.

The study also explored the effect of polypropylene fibers on reducing strength loss, frost heave, and thaw settlement during freeze–thaw (F–T) cycles, finding that the strength reduction was limited to 18% when 1% fibers were incorporated, compared with 51% in unreinforced samples. This aligns with the study by Cai et al. [59], which similarly reported that fiber reinforcement mitigates the detrimental effects of freeze–thaw cycles on clayey soils. In addition, fiber inclusion improved resistance to volumetric changes caused by F–T cycles, indicating that 1% reinforcement provides the most effective resistance to these effects.

The results suggest that incorporating polypropylene fibers can improve soil durability by mitigating volumetric changes and maintaining structural integrity during freeze–thaw (F–T) cycles. Additionally, due to the inert nature of polypropylene and its minimal environmental impact, its use is highly suitable for long-term projects. A fiber content of

1% has been found to be optimal for resisting these effects. However, it is important to note that the study only investigated up to 10 freeze–thaw cycles, and further research is needed to assess the long-term performance of fiber-reinforced soils under more extensive freeze–thaw conditions.

Author Contributions: Data curation, T.T. and Y.S.U.; Investigation, T.T.; Resources, T.T. and Y.S.U.; Validation, T.T. and Y.S.U.; Visualization, T.T.; Writing—review and editing, T.T. and Y.S.U. All authors have read and agreed to the published version of the manuscript.

Funding: This research received no external funding.

Institutional Review Board Statement: Not applicable.

Informed Consent Statement: Not applicable.

Data Availability Statement: All data, models, and code generated or used during the study appear in the submitted article.

Conflicts of Interest: The authors declare that they have no known conflicts of interest or personal relationships that could have appeared to influence the work reported in this paper.

References

1. Hohmann-Porebska, M. Micro fabric effects in frozen clays in relation to geotechnical parameters. *Appl. Clay Sci.* **2002**, *21*, 77–87. [CrossRef]
2. Miller, C.J.; Mi, H.; Yesiller, N. Experimental analysis of desiccation crack propagation in clay liners. *J. Am. Water Resour. Assoc. (JAWRA)* **1998**, *34*, 677–686. [CrossRef]
3. Baker, R., Sr. Tensile strength, tension cracks, and stability of slopes. *Soils Found.* **1981**, *21*, 1–17. [CrossRef]
4. Silvestri, V.; Sarkis, G.; Bekkouche, N.; Soulié, M. Evapotranspiration, trees and damage to foundations in sensitive clays. In *Proceedings of the Canadian Geotechnical Conference*; Canadian Geotechnical Society: Surrey, BC, Canda, 1992; Volume II, pp. 533–538.
5. Ghazavi, M.; Roustaei, M. The influence of freeze-thaw cycles on the unconfined compressive strength of fiber-reinforced clay. *Cold Reg. Sci. Technol.* **2010**, *61*, 125–131. [CrossRef]
6. Roustaei, M.; Eslami, A.; Ghazavi, M. Effects of freeze thaw cycles on a fiber reinforced fine grained soil in relation to geotechnical parameters. *Cold Reg. Sci. Technol.* **2015**, *120*, 127–137. [CrossRef]
7. Akbulut, S.; Arasan, S.; Kalkan, E. Modification of clayey soils using scrap tire rubber and synthetic fibers. *Appl. Clay Sci.* **2007**, *38*, 23–32. [CrossRef]
8. AlZubaidi, R.M.; AlRawi, K.H.; AlFalahi, A.J. Using cement dust to reduce swelling of expansive soil. *Geomech. Eng.* **2013**, *5*, 565–574. [CrossRef]
9. Al-Mahbashi, A.M.; Elkady, T.Y.; Alrefeai, T.O. Soil water characteristic curve and improvement in lime treated expansive soil. *Geomech. Eng.* **2015**, *8*, 687–696. [CrossRef]
10. Sharo, A.A.; Alhowaidi, Y.A.; Al-Tawaha, M.S. Improving Properties of Expansive Soil Using Cement, Quick Lime and Cement-Lime Blend. *Int. Rev. Civ. Eng.* **2019**, *10*, 94. [CrossRef]
11. Mohammed, A.M.A.; Indra, S.H.H.; Aminaton, M.; Seyed, V.A.; Zahiraniza, M.; Montasir, O.A.A. Mechanical behaviour of waste powdered tiles and Portland cement treated soft clay. *Geomech. Eng.* **2019**, *19*, 37–47. [CrossRef]
12. Farghaly, A.A.; El-Shater, A.; Naiem, M.A.A.; Hamdy, F. Lime addition chemical stabilization of expansive soil at Al-Kawamil city, Sohag region, Egypt. *Adv. Comput. Des.* **2020**, *5*, 1–11. [CrossRef]
13. Kumar, A.; Walia, B.S.; Bajaj, A. Influence of fly ash, lime, and polyester fibers on compaction and strength properties of expansive soil. *J. Mater. Civ. Eng.* **2007**, *19*, 242–248. [CrossRef]
14. Babu, G.L.S.; Vasudevan, A.K. Strength and stiffness response of coir fiber-reinforced tropical soil. *J. Mater. Civ. Eng.* **2008**, *20*, 571–577. [CrossRef]
15. Viswanadham, B.V.S.; Phanikumar, B.R.; Mukherjee, R.V. Swelling behaviour of a geofiber-reinforced expansive soil. *Geotext. Geomembr.* **2009**, *27*, 73–76. [CrossRef]
16. Tang, C.; Wang, D.; Cui, Y.; Shi, B.; Li, J. Tensile strength of fiber-reinforced soil. *J. Mater. Civ. Eng.* **2016**, *28*, 04016031. [CrossRef]
17. Taleb, T.; Unsever, Y.S. Study on Strength and Swell Behavioral Change and Properties of the Clay–Fiber Mixtures. *Sustainability* **2022**, *14*, 6767. [CrossRef]
18. Taleb, T.; Unsever, Y.S. Evaluation of high plasticity clay stabilization methods for resisting the environmental changes. *Geomech. Eng.* **2022**, *30*, 461–469. [CrossRef]

19. Aldaood, A.; Bouasker, M.; Al-Mukhtar, M. Impact of freeze thaw cycles on mechanical behaviour of lime stabilized gypseous soils. *Cold Reg. Sci. Technol.* **2014**, *99*, 38–45. [CrossRef]
20. Ling, X.; Tian, S.; Tang, L.; Li, S. A damage-softening and dilatancy prediction model of coarse-grained materials considering freeze thaw effects. *Transp. Geotech.* **2020**, *22*, 100307. [CrossRef]
21. Boz, A.; Sezer, A. Influence of fiber type and content on freeze-thaw resistance of fiber reinforced lime stabilized clay. *Cold Reg. Sci. Technol.* **2018**, *151*, 359–366. [CrossRef]
22. Ding, M.; Zhang, F.; Ling, X.; Lin, B. Effects of freeze-thaw cycles on mechanical properties of polypropylene fiber and cement stabilized clay. *Cold Reg. Sci. Technol.* **2018**, *154*, 155–165. [CrossRef]
23. Zhang, Y.; Johnson, A.E.; White, D.J. Laboratory freeze thaw assessment of cement, fly ash, and fiber stabilized pavement foundation materials. *Cold Reg. Sci. Technol.* **2016**, *122*, 50–57. [CrossRef]
24. Zhang, Y.; Johnson, A.E.; White, D.J. Freeze-thaw performance of cement and fly ash stabilized loess. *Transp. Geotech.* **2019**, *21*, 100279. [CrossRef]
25. Hejazi, S.M.; Sheikhzadeh, M.; Abtahi, S.M.; Zadhoush, A. A simple review of soil reinforcement by using natural and synthetic fibers. *Constr. Build. Mater.* **2012**, *30*, 100–116. [CrossRef]
26. Zhao, R.; Zhang, S.; He, J.; Gao, W.; Jin, D.; Xie, L. Experimental study on freezing and thawing deformation of geogrid-reinforced silty clay structure. *Bull. Eng. Geol. Environ.* **2020**, *79*, 2883–2892. [CrossRef]
27. Soltani-Jigheh, H.; Azarnia, A. Effect of liquid polymeric and lime additives on the behavior of fine-grained soil at unfrozen and freeze-thaw conditions. *Indian Geotech. J.* **2017**, *47*, 529–536. [CrossRef]
28. Krainiukov, A.; Liu, J.; Kravchenko, E.; Chang, D. Performance of silty sand reinforced with aqueous solution of polyvinyl alcohol subjected to freeze-thaw cycles. *Cold Reg. Sci. Technol.* **2020**, *174*, 103054. [CrossRef]
29. Eskisar, T.; Altun, S.; Kalıpcılar, I. Assessment of strength development and freeze thaw performance of cement treated clays at different water contents. *Cold Reg. Sci. Technol.* **2015**, *111*, 50–59. [CrossRef]
30. Zaimoglu, A.S. Freezing-thawing behavior of fine-grained soils reinforced with polypropylene fibers. *Cold Reg. Sci. Technol.* **2010**, *60*, 63–65. [CrossRef]
31. Ghazavi, M.; Roustaei, M. Freeze-thaw performance of clayey soil reinforced with geotextile layer. *Cold Reg. Sci. Technol.* **2013**, *89*, 22–29. [CrossRef]
32. Orakoglu, M.E.; Liu, J. Effect of freeze-thaw cycles on triaxial strength properties of fiber-reinforced clayey soil. *KSCE J. Civ. Eng.* **2017**, *21*, 2128–2140. [CrossRef]
33. Kravchenko, E.; Liu, J.; Krainiukov, A.; Chang, D. Dynamic behavior of clay modified with polypropylene fiber under freeze-thaw cycles. *Transp. Geotech.* **2019**, *21*, 100282. [CrossRef]
34. Yarbasi, N.; Kalkan, E.; Akbulut, S. Modification of the geotechnical properties, as influenced by freeze thaw, of granular soils with waste additives. *Cold Reg. Sci. Technol.* **2007**, *48*, 44–54. [CrossRef]
35. Kalkan, E. Effects of silica fume on the geotechnical properties of fine-grained soils exposed to freeze and thaw. *Cold Reg. Sci. Technol.* **2009**, *58*, 130–135. [CrossRef]
36. Ahmadi, S.; Ghasemzadeh, H.; Changizi, F. Effects of thermal cycles on microstructural and functional properties of nano treated clayey soil. *Eng. Geol.* **2021**, *280*, 105929. [CrossRef]
37. Jafari, M.; Esna-Ashari, M. Effect of waste tire cord reinforcement on unconfined compressive strength of lime stabilized clayey soil under freeze-thaw condition. *Cold Reg. Sci. Technol.* **2012**, *82*, 21–29. [CrossRef]
38. Gao, C.; Du, G.; Guo, Q.; Xia, H.; Pan, H.; Cai, J. Dynamic and static splitting tensile properties of basalt fiber reinforced cemented clay under freeze-thaw cycles. *J. Mater. Civ. Eng.* **2020**, *32*, 06020014. [CrossRef]
39. Rogers, C.D.; Thomas, A.M.; Jefferson, I.; Gaterell, M. Carbon dioxide emissions due to highway subgrade improvements. *Transp. Res. Rec. J. Transp. Res. Board* **2009**, *2104*, 80–87. [CrossRef]
40. Caravaca, F.; Lozano, Z.; Rodríguez-Caballero, G.; Rold, A. Spatial shifts in soil microbial activity and degradation of pasture cover caused by prolonged exposure to cement dust. *Land Degrad. Dev.* **2017**, *28*, 1329–1335. [CrossRef]
41. El-Attar, M.M.; Sadek, D.M.; Salah, A.M. Recycling of high volumes of cement kiln dust in bricks industry. *J. Clean. Prod.* **2017**, *143*, 506–515. [CrossRef]
42. Hu, Z.; Yang, Y.; Zhang, H. Durability and damage evolution of steel fiber and Nano-SiO_2 reinforced concrete under freeze-thaw and salt erosion environments based on acoustic emission and Computed Tomography analysis. *J. Build. Eng.* **2025**, *115*, 114595. [CrossRef]
43. Liu, Z.; Qi, X.; Shui, Z. Enhancing the toughness of ultra-high performance concrete through improved fiber-matrix interface bonding. *Constr. Build. Mater.* **2025**, *491*, 142616. [CrossRef]
44. Brown, R.; Shukla, A.; Natarajan, K.R. *Fiber Reinforcement of Concrete Structures*; University of Rhode Island Trans Center: Kingston, RI, USA, 2002.
45. Franklin Associates. *Life Cycle Impacts for Postconsumer Recycled Resins: PET, HDPE, and PP*; A Division of Eastern Research Group (ERG): Concord, MA, USA, 2018.

46. Taleb, T.; Unsever, Y.S. Effect of Polypropylene Fibers on Physical and Strength Properties of Local Clayey Soil. In *Proceedings of 14th International Congress on Advances in Civil Engineering*; Yildiz Technical University (YTU) Press: Istanbul, Turkey, 2021; pp. 611–618.
47. *ASTM D2850-25*; Standard Test Method for Unconsolidated-Undrained Triaxial Compression Test on Cohesive Soils. ASTM International: West Conshohocken, PA, USA, 2025.
48. Shukla, S.K. Engineering Behaviour of Fibre-Reinforced Soil. In *Fundamentals of Fibre-Reinforced Soil Engineering*; Springer: Singapore, 2017; pp. 45–110. [CrossRef]
49. Isazadeh-Khiav, B.; Akhlaghi, T.; Hajialilue-Bonab, M. Studying the Failure Behavior of Cement-fiber-treated Sand under Triaxial Direct Tension Tests. *Period. Polytech. Civ. Eng.* **2022**, *66*, 384–397. [CrossRef]
50. Hong, Y.; Zhou, Q.; Ma, W.; Niu, B.; Liu, F.; Chen, Q. Effects of freezing and thawing on soil shear strength in the western farming pastoral ecotone of northern China. *Sci. Rep.* **2025**, *15*, 23150. [CrossRef] [PubMed]
51. Rosa, M.G.; Cetin, B.; Edil, T.B.; Benson, C.H. Development of a Test Procedure for Freeze-Thaw Durability of Geomaterials Stabilized With Fly Ash. *Geotech. Test. J.* **2016**, *39*, 938–953. [CrossRef]
52. AlFukaha, R.; Shaqour, F.; Ismeik, M. Freeze-thaw durability of clayey soils stabilized by alkaline-activated kaolin and recycled cement kiln dust. *Results Eng.* **2024**, *24*, 103199. [CrossRef]
53. Wang, D.; Ma, W.; Niu, Y.H.; Chang, X.; Wen, Z. Effects of cyclic freezing and thawing on mechanical properties of Qinghai–Tibet clay. *Cold Reg. Sci. Technol.* **2007**, *48*, 34–43. [CrossRef]
54. Andersland, O.B.; Ladanyi, B. *Frozen Ground Engineering*, 2nd ed.; American Society of Civil Engineers (ASCE Press): Reston, VA, USA; John Wiley & Sons: New York, NY, USA, 2004.
55. Tong, L.; Fu, L.; Wu, B.; Xu, C.; Lim, C.W. Packing fraction effect on dynamic creep deformation of granular materials. *Acta Geotech.* **2025**, *20*, 2135–2144. [CrossRef]
56. Zhao, R.; Chang, H.; Yu, J.; Huang, D.; Yang, D.; Yang, H.; Zhou, L. The influence of freeze-thaw action and particle size characteristics on the shear resistance of black soil. *Sci. Rep.* **2026**, *16*, 6176. [CrossRef]
57. Wei, L.; Chai, S.X.; Zhang, H.Y.; Shi, Q. Mechanical properties of soil reinforced with both lime and four kinds of fiber. *Constr. Build. Mater.* **2018**, *172*, 300–308. [CrossRef]
58. Consoli, N.C.; Foppa, D.; Festugato, L.; Heineck, K.S. Key Parameters for strength control of artificially cemented soils. *J. Geotech. Geoenviron. Eng.* **2007**, *133*, 197–205. [CrossRef]
59. Cai, Y.; Shi, B.; Ng, C.W.; Tang, C.-S. Effect of Polypropylene Fibre and Lime Admixture on Engineering Properties of Clayey Soil. *Eng. Geol.* **2006**, *87*, 230–240. [CrossRef]

Disclaimer/Publisher's Note: The statements, opinions and data contained in all publications are solely those of the individual author(s) and contributor(s) and not of MDPI and/or the editor(s). MDPI and/or the editor(s) disclaim responsibility for any injury to people or property resulting from any ideas, methods, instructions or products referred to in the content.